Sensors and Materials, Vol. 38, No. 6 (2026) 3023–3032
MYU Tokyo

S & M 4485

Effects of Al, Mo, and Ag Interlayers on the Optoelectronic Properties of SnO_2/Metal/ZnO Multilayer Transparent Conductive Films

Yun Ho and Tao-Hsing Chen*

Department of Mechanical Engineering, National Kaohsiung University of Science and Technology, Kaohsiung City 807, Taiwan, No. 415, Jiangong Rd., Sanmin Dist., Kaohsiung City 807618, Taiwan

(Received March 2, 2026; accepted April 10, 2026)

Keywords: SnO_2, electrical property, RF sputtering, optical property, oxygen flow rate

SnO_2/metal/ZnO multilayer transparent conductive films incorporating Ag, Al, and Mo interlayers were fabricated by RF and DC magnetron sputtering to investigate the effects of interlayer metal selection on structural, electrical, and optical properties. Postdeposition vacuum annealing was performed at temperatures ranging from 200 to 500 °C. Film thickness, crystallinity, carrier transport behavior, optical transmittance, grain size, and figure of merit (FOM) were systematically analyzed. X-ray diffraction results revealed enhanced crystallinity with increasing annealing temperature, accompanied by grain growth and phase evolution. Hall measurements indicated that optimal electrical performance was achieved by 200 °C annealing for Ag and Mo interlayers, with resistivities of 3.60×10^{-2} and 4.02×10^{-2} Ω·cm, respectively. Optical measurements showed an average visible transmittance exceeding 80% after 400 °C annealing for all samples. Among the investigated structures, the SnO_2/Mo/ZnO film annealed at 200 °C exhibited the highest FOM of 9.42×10^{-5} Ω^{-1}, demonstrating balanced electrical conductivity and optical transparency. The results confirm that appropriate interlayer engineering effectively enhances the optoelectronic performance of oxide/metal/oxide multilayer films for transparent electrode- and sensor-related applications.

1. Introduction

Transparent conducting oxides (TCOs) simultaneously exhibit high electrical conductivity and optical transparency, making them essential materials for solar cells, flat-panel displays, thin-film transistors, and optoelectronic sensors. Conventional metal films exhibit excellent conductivity but limited transparency owing to strong reflection in the visible and infrared regions. To achieve both transparency and conductivity, oxide/metal/oxide (OMO) multilayer structures have been widely developed.[1–9]

SnO_2 is a wide-bandgap semiconductor (>3 eV) with high chemical stability and good optical transparency. However, its conductivity is generally inferior to that of metallic films. Introducing a thin metallic interlayer between oxide layers can significantly enhance carrier transport while

*Corresponding author: e-mail: thchen@nkust.edu.tw
https://doi.org/10.18494/SAM6312

ISSN 0914-4935
https://myukk.org/

maintaining optical performance. Nevertheless, the electrical and optical properties strongly depend on the type of interlayer metal and postdeposition thermal treatment.[10–15]

In this study, SnO_2/metal/ZnO multilayer films with Ag, Al, and Mo interlayers were prepared. The effects of annealing temperature on crystallinity, carrier concentration, mobility, transmittance, grain growth, and figure of merit (FOM) were systematically investigated.[16–20]

2. Experimental Procedure

SnO_2 films were deposited on glass substrates by RF magnetron sputtering (I-Shien Corporation) using a 99.99% pure SnO_2 target. The sputtering power was 80 W with an Ar/O_2 gas flow rate of 30/5 sccm at a working pressure of 6 mTorr for 30 min. Subsequently, metallic interlayers (Ag, Al, and Mo; 99.99% purity) were deposited by DC magnetron sputtering at 20 W with an Ar flow rate of 15 sccm and a working pressure of 10 mTorr for 1 min. Finally, ZnO top layers were deposited by RF sputtering under 80 W power with an Ar flow rate of 30 sccm at 6 mTorr for 30 min, forming SnO_2/metal/ZnO multilayer structures. Postdeposition vacuum annealing was conducted at 200, 300, 400, and 500 ℃. Finally, the properties of each layer were measured individually. The crystal structure was analyzed by X-ray diffraction (XRD, D8 ADVANCE ECO, Bruker) and electrical properties were measured by Hall measurement (Nanomagnetics Instruments). The optical transmittance was obtained by UV–Vis spectroscopy (U-2900, Hitachi company).

3. Results and Discussion

3.1 Crystal structure properties

Figures 1(a) to 1(c) present the XRD analysis results, which showed that all multilayer films began to exhibit pronounced diffraction peaks corresponding to the (101) plane near $2\theta \approx 34°$ after annealing at 200 ℃, indicating improved crystallinity. At higher annealing temperatures, additional peaks near 27° associated with mixed SnO and SnO_2 phases were observed. For Mo interlayers, a Mo oxide (220) peak appeared near 52° after 300 ℃ annealing. Ag and Al interlayers exhibited oxide-related peaks at higher annealing temperatures, indicating oxidation at elevated temperatures. Grain size was calculated using the Scherrer equation. Grain growth became significant above 300 ℃, and the Mo-interlayer sample showed the most pronounced grain enlargement, reaching 84.12 nm at 500 ℃. The thickness of SnO_2 was about 90 nm and thst of each metal thin film was about 20 nm. The total thickness of each multilayer of thin films was about 220 nm.

3.2 Analysis of electrical properties

The electrical performance strongly depends on both the interlayer type and the annealing temperature. Tables 1 to 3 present the results of the electrical analysis of SnO_2/Ag/ZnO, SnO_2/Al/ZnO, and SnO_2/Mo/ZnO multilayer films prepared with different annealing temperatures.

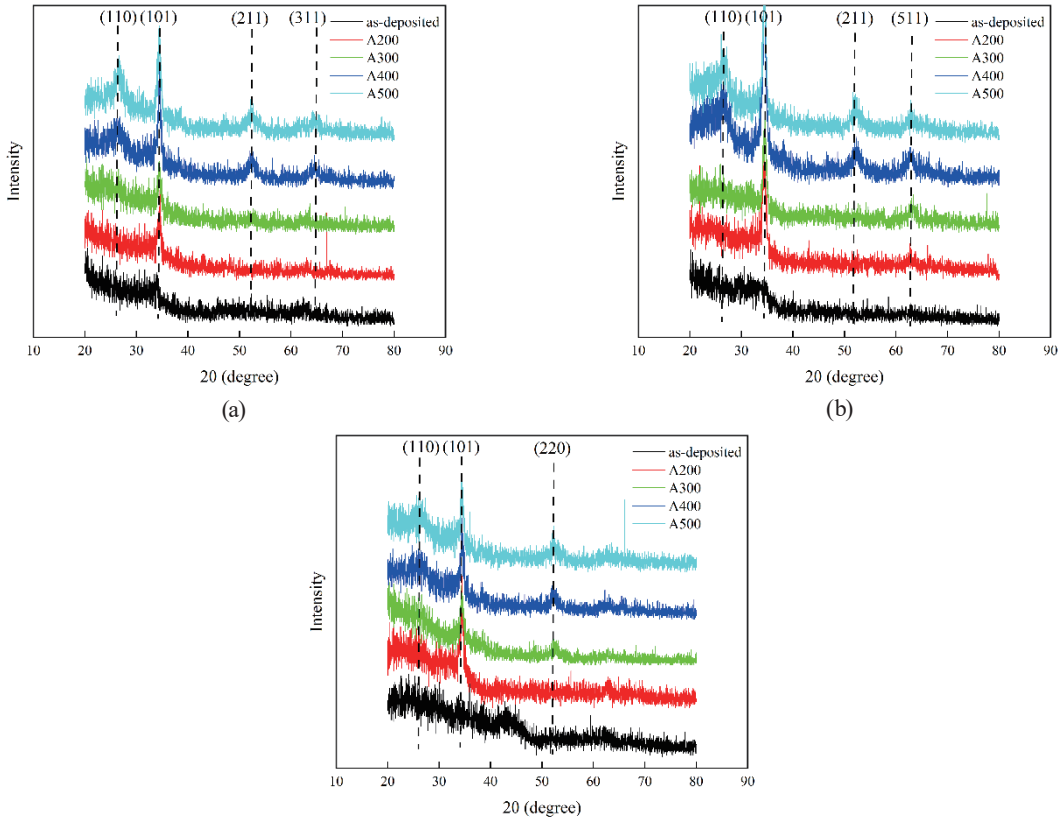

Fig. 1. (Color online) XRD analysis results of (a) SnO_2/Ag/ZnO, (b) SnO_2/Al/ZnO, and (c) SnO_2/Mo/ZnO at different annealing temperatures.

Table 1
Electrical properties of SnO_2/Ag/ZnO prepared at different annealing temperatures.

SnO_2/Ag/ZnO electrical property			
Annealing temperature (°C)	Resistivity (Ω-cm)	Mobility (cm^2/Vs)	Carrier concentration (cm^{-3})
as-deposited	1.74E−01	2.75E+00	1.30E+19
200	3.60E−02	1.32E+00	1.31E+20
300	4.25E−02	2.83E−01	5.20E+20
400	1.91E+01	1.28E−02	2.54E+19
500	8.81E+00	2.03E+00	3.49E+17

Table 2
Electrical properties of SnO_2/Al/ZnO prepared at different annealing temperatures.

SnO_2/Al/ZnO electrical property			
Annealing temperature (°C)	Resistivity (Ω-cm)	Mobility (cm^2/Vs)	Carrier concentration (cm^{-3})
as-deposited	9.38E−02	1.77E+00	3.75E+19
200	1.65E−01	1.18E+00	3.21E+19
300	2.16E−01	2.47E−01	1.17E+20
400	9.37E+01	2.26E−02	2.95E+18
500	1.48E+01	1.32E−02	3.19E+19

Table 3
Electrical properties of SnO_2/Mo/ZnO prepared at different annealing temperatures.

SnO_2/Mo/ZnO electrical property			
Annealing temperature (°C)	Resistivity (Ω-cm)	Mobility (cm^2/Vs)	Carrier concentration (cm^{-3})
as-deposited	5.03E−02	2.33E+00	5.31E+19
200	4.02E−02	3.50E+00	4.43E+19
300	4.12E−01	8.51E−01	1.78E+19
400	1.89E+00	1.12E−01	2.96E+19
500	1.24E+02	1.58E−03	3.18E+19

From Table 1, it can be seen that the SnO_2/Ag/ZnO multilayer films annealed at 200 °C exhibited the lowest resistivity (3.60×10^{-2} Ω·cm). This improvement is attributed to the high intrinsic conductivity of Ag. The Ag thin film has an increased carrier concentration (~10^{20} cm^{-3}) and a reduced interface resistance after low-temperature annealing. However, at temperatures ≥400 °C, the resistivity increased markedly. This behavior is likely due to Ag agglomeration, leading to discontinuous conductive pathways and enhanced carrier scattering.

The as-deposited SnO_2/Al/ZnO sample exhibited a relatively low resistivity of 9.38×10^{-2} Ω·cm. However, annealing above 300 °C significantly increased the resistivity up to 10^1 Ω·cm. This deterioration is attributed to the rapid oxidation of Al, resulting in the formation of insulating Al_2O_3 phases. The formation of this oxide barrier layer impedes electron transport across interfaces, increasing the resistivity despite the improved crystallinity.

The SnO_2/Mo/ZnO structure annealed at 200 °C achieved balanced electrical performance with a resistivity of 4.02×10^{-2} Ω·cm and a mobility of 3.50 cm^2/V·s. The superior performance of Mo can be attributed to the moderate electrical conductivity and higher oxidation resistance of Mo than Al, and a reduced agglomeration tendency of Mo compared with Ag. Thus, Mo provides a more thermally stable interlayer under moderate annealing conditions.

3.3 Analysis of transmittance and optical properties

Figures 2–4 show the transmittance results. It can be observed that all samples exhibited increasing averages. This trend can be explained by the reduced light scattering owing to the improved crystallinity and the decrease in metallic reflectance as interlayers partially oxidize. The optical bandgap *Eg* can also represent film transparency. The optical bandgap values were consistently above 3 eV, confirming wide-bandgap semiconductor behavior. The slight bandgap widening after annealing may be associated with the reduced defect density and possible Burstein–Moss effect due to the increased carrier concentration:[21,22]

$$(\alpha h\upsilon)^2 = A(h\upsilon - Eg), \tag{1}$$

where A is a constant, α is the absorption coefficient, and $h\upsilon$ is the incident photon energy. Figures 5–7 show the bandgap values at different annealing temperatures for the different multilayer thin films. Importantly, no marked bandgap shifts were observed, indicating that

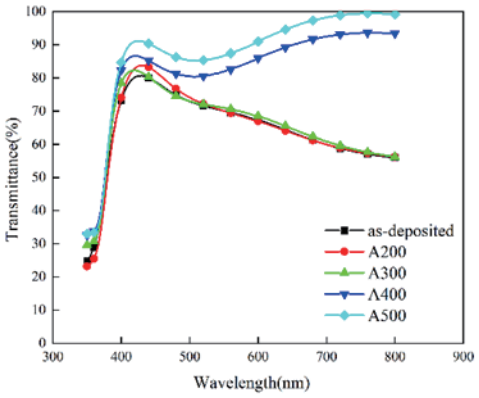

Fig. 2. (Color online) Optical transmittance of SnO_2/Ag/ZnO prepared at different annealing temperatures.

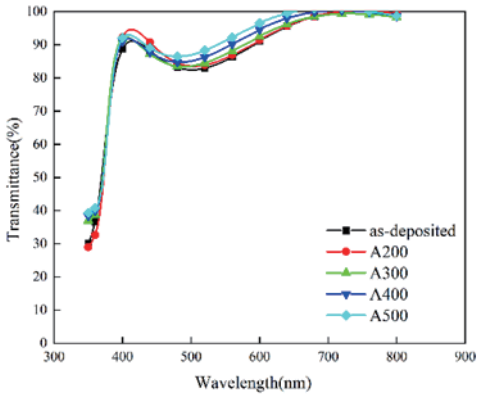

Fig. 3. (Color online) Optical transmittance of SnO_2/Al/ZnO prepared at different annealing temperatures.

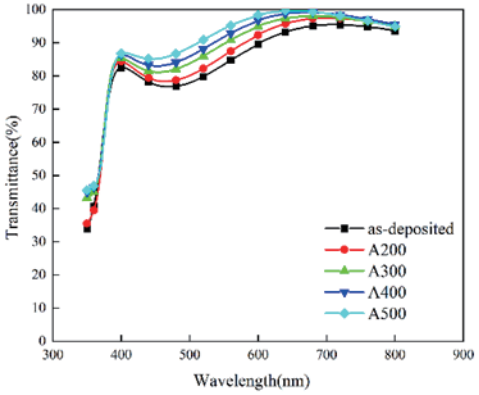

Fig. 4. (Color online) Optical transmittance of SnO_2/Mo/ZnO prepared at different annealing temperatures.

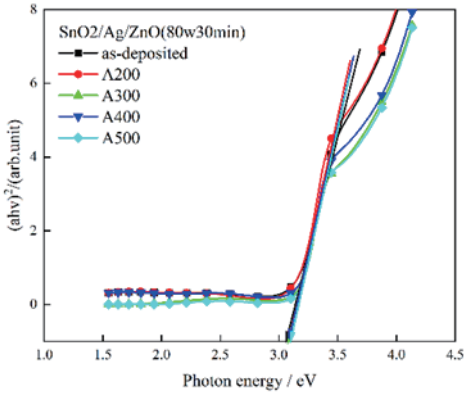

Fig. 5. (Color online) Bandgap values of SnO_2/Ag/ZnO prepared at different annealing temperatures.

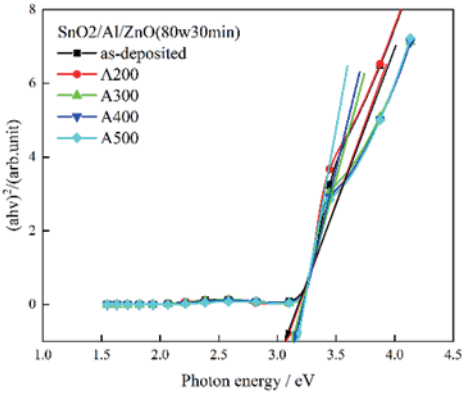

Fig. 6. (Color online) Bandgap values of SnO_2/Al/ZnO prepared at different annealing temperatures.

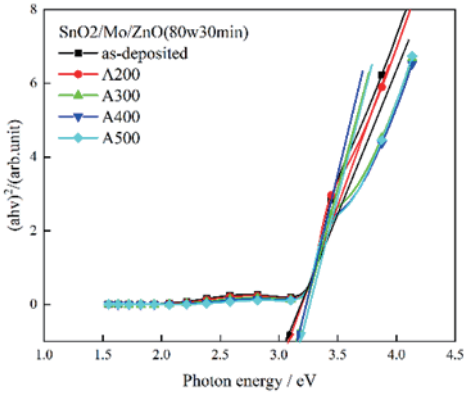

Fig. 7. (Color online) Bandgap values of SnO_2/Mo/ZnO prepared at different annealing temperatures.

interlayer engineering primarily affects electrical transport rather than the fundamental electronic structure.

3.4 Analysis of crystal size

Grain size, calculated using the Scherrer equation, increased with annealing temperature for all multilayer structures. This grain coarsening is associated with reduced grain boundary density and lower grain boundary scattering.[23]

$$D = \frac{0.9\lambda}{\beta \cos\theta} \tag{2}$$

Here, D is the grain size, λ is the X-ray incident angle (0.15418 nm), θ is the incident angle, and β is the full width at half maximum (*FWHM*). Tables 4–6 present the crystal grain sizes for all multilayer thin films prepared at different annealing temperatures.

The Mo-interlayer sample demonstrated the most significant grain growth, reaching 84.12 nm after annealing at 500 °C, indicating enhanced atomic diffusion and lattice rearrangement. This suggests that phase evolution (SnO formation) and interlayer oxidation play dominant roles at higher temperatures. Therefore, optimal electrical performance is achieved with a moderate annealing temperature (200 °C), where crystallinity improves without excessive phase transformation.

Table 4
Effect of annealing temperature on the grain size of SnO_2/Ag/ZnO.

SnO_2/Ag/ZnO		
Annealing temperature (°C)	*FWHM*	Grain size (nm)
300	0.203	41.00
400	0.186	44.74
500	0.169	49.25

Table 5
Effect of annealing temperature on the grain size of SnO_2/Al/ZnO.

SnO_2/Al/ZnO		
Annealing temperature (°C)	*FWHM*	Grain size (nm)
300	0.293	28.41
400	0.234	35.58
500	0.227	36.67

Table 6
Effect of annealing temperature on the grain size of SnO_2/Mo/ZnO.

SnO_2/Mo/ZnO		
Annealing temperature (°C)	*FWHM*	Grain size (nm)
300	0.194	42.91
400	0.128	65.01
500	0.099	84.12

3.5 FOM analysis

The performance of TCO films is often evaluated using FOM, defined by the ratio of transmittance to resistance:[24–26]

$$\varnothing_{TC} = \frac{T_{av}^{10}}{R_{sh}}, \tag{3}$$

where T_{av} is the average optical transmittance and R_{sh} is the sheet resistance expressed in Ω^{-1}. Figures 8–10 present FOM values of all SnO_2/Ag/ZnO multilayer thin films. SnO_2/Mo/ZnO annealed at 200 °C achieved the highest FOM (9.42×10^{-5} Ω^{-1}). SnO_2/Ag/ZnO showed strong electrical performance but lower FOM owing to lower transmittance. However, SnO_2/Ag/ZnO had the intermediate FOM. The superior FOM of the Mo-interlayer structure originates from sufficient carrier mobility, stable interface formation, and maintained optical transparency. This

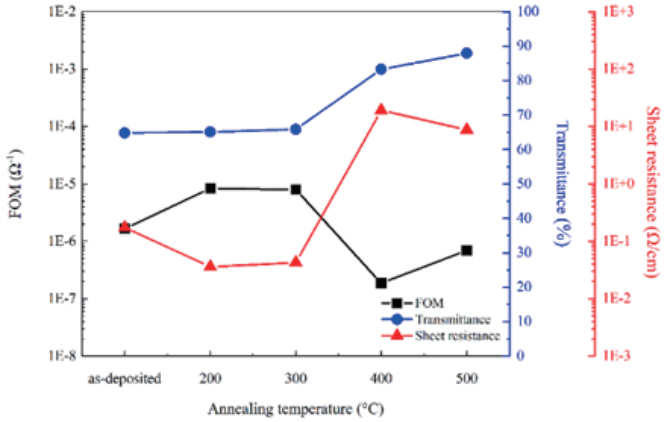

Fig. 8. (Color online) FOM of SnO_2/Ag/ZnO thin films prepared at different annealing temperatures.

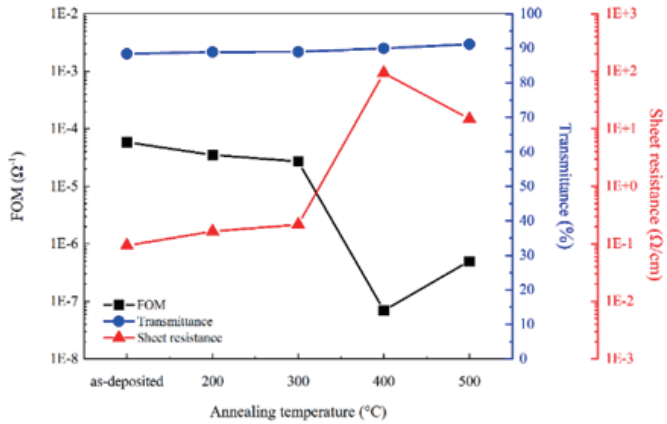

Fig. 9. (Color online) FOM of SnO_2/Al/ZnO thin films prepared at different annealing temperatures.

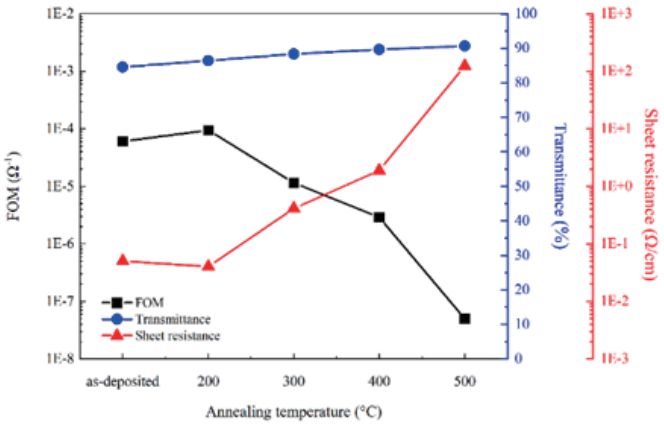

Fig. 10. (Color online) FOM of SnO_2/Mo/ZnO thin films prepared at different annealing temperatures.

demonstrates that electrical conductivity alone does not determine overall performance. Instead, optimal transparent conductive behavior requires a careful control of interlayer oxidation kinetics, crystallinity, and carrier scattering mechanisms.

4. Conclusions

SnO_2/metal/ZnO multilayer transparent conductive films with Ag, Al, and Mo interlayers were successfully fabricated and systematically investigated.

(1) Annealing at 200 ℃ significantly improved crystallinity and electrical conductivity.

(2) Optical transmittance exceeding 80% was achieved after 400 ℃ annealing.

(3) Grain size increased with annealing temperature owing to recrystallization.

(4) The SnO_2/Mo/ZnO film annealed at 200 ℃ exhibited the highest FOM of 9.42×10^{-5} Ω^{-1}.

These results demonstrate that Mo interlayers prepared under optimized annealing conditions provide superior optoelectronic performance, making the multilayer structure promising for transparent electrode and sensor applications.

Acknowledgments

This paper was completed as part of Research Project NSTC114-2637-E-992 -004, which is supported by the National Science and Technology Council of Taiwan. The authors would like to express their gratitude to the National Science and Technology Council for its support, which enabled the smooth completion of this research. The authors also gratefully acknowledge the use of EM000700 of NSTC 114-2731-M-006-001 belonging to the Core Facility Centre of National Cheng Kung University.

References

1 C. H. Yu, S. T. Wicaksono, S. T. Wang, and T. H. Chen: Sens. Mater. **37** (2025) 1825. https://doi.org/10.18494/SAM5316
2 T. H. Chen and C. L. Yang: Opt. Quant. Electron. **48** (2016) 533. https://doi.org/10.1007/s11082-016-0808-3
3 K. J. Ko, S. R. Shin, H .B. Lee, E. Jeong, Y. J. Yoo, H. M. Kim, Y. M. Song, J. Yun, and J. W. Kang: Materi. Today Energy **20** (2021) 100704. https://doi.org/10.1016/j.mtener.2021.100704
4 T. H. Chen, C. C. Chiang, and T. Y. Chen.: Microsyst. Technol. **32** (2017) 1687. https://doi.org/10.1007/s00542-015-2689-y
5 W. N. Wang, T. D. Chang, and T. H. Chen: Sens. Mater. **36** (2024) 3757. https://doi.org/10.18494/SAM5049
6 P. Zhao, S. Kim, S. Yoon, and P. Song: Thin Solid Films **665** (2018) 137. https://doi.org/10.1016/j.tsf.2018.09.018Get rights and content
7 Y. Cho, N.S. Parmar, S. Nahm, and J. W. Choi: J. Alloys Comp. **694** (2017) 217. https://doi.org/10.1016/j.jallcom.2016.09.293
8 T. H. Chen, C. C. Chiang, and T. Y. Chen.: Microsyst. Technol. **32** (2017) 1687. https://doi.org/10.1007/s00542-015-2689-y
9 M. Purica, E. Budianu, E. Rusu, M Danila, and R. Gavrila: Thin Solid Films **403**–**404** (2002) 485. https://doi.org/10.1016/S0040-6090(01)01544-9
10 N. Sajdeh, S. A. A. Terohid, S. Asgary, and G Behzad: Phys. Scripta **99** (2024) 095977. https://doi.org/10.1088/1402-4896/ad6aa2
11 M. Mishra, S. K. Singh, and M. Kumar: MRS Advances **10** (2025) 2360. https://doi.org/10.1557/s43580-025-01329-1
12 T. B. Raju, B. R. Kumar, and Y. Ramakrishna: Braz. J. Phys. **54** (2024) 238. https://doi.org/10.1007/s13538-024-01620-w
13 A. S. Yusuf, M. Markwitz, Z. Chen, M. Ramezani, J. V. Kennedy, and H. Fiedler: Surf. Interfaces **55** (2024) 105325. https://doi.org/10.1016/j.surfin.2024.105325
14 C. F. Liu, T. H. Chen, and Y. S. Huang: Sen. Mater. **32** (2020) 2321. https://doi.org/10.18494/SAM.2020.2867
15 T. H. Chen , M. W. Wang, C. L. Yang, and Y. S. Huang: Microsyst. Technol. **25** (2019) 2109. https://doi.org/10.1007/s00542-019-04360-z
16 M. Y. Yen, T. H. Chen, P. H. Lai, S. L. Tu, and Y. H. Shen: Sen. Mater. **33** (2021) 3941. https://doi.org/10.18494/SAM.2021.3706
17 M. N. A. Bitu, N. I. Tanvir, S. Islam, and S. F. U. Farhad: MRS Advances **8** (2023) 194. https://doi.org/10.1557/s43580-023-00515-3
18 S. R. Vanga, V. Sarada, and A. B. Yadav: Appl. Phys. A **131** (2025) 360. https://doi.org/10.1007/s00339-025-08481-3.
19 C. F. Liu, S. C. Shi, T. H. Chen, and G. L. Guo: Sens. Mater. **34** (2022) 4127. https://doi.org/10.18494/SAM4133
20 A. K. Gangwar, R. Godiwal, J. Jaiswal, V. Baloria, P. Pal, G. Gupta, and P. Singh: Vacuum **177** (2020) 109353. https://doi.org/10.1016/j.vacuum.2020.109353
21 T. Minami, H. Nanto, and S. Takata: J. Appl. Phys. **24** (1985) L605. https://doi.org/10.1143/JJAP.24.L605
22 Y. C. Chang, T. H. Chen, T. D. Chang, S. L. Tu, and Y. H. Shen: Sens. Mater. **35** (2023) 2871. https://doi.org/10.18494/SAM4354
23 M. Caglar, S. Ilican, and Y Caglar: Thin Solid Films **517** (2009) 5023. https://doi.org/10.1016/j.tsf.2009.03.037
24 T. H. Chen and H. D. Su: Sens. Mater. **30** (2018) 2541. https://doi.org/10.18494/SAM.2018.2056
25 C. Y. Lin, T. H. Chen, S .L.Tu, Y. H Shen, and J. T. Huang: Opt. Quant. Electron **50** (2018) 169. https://doi.org/10.1007/s11082-018-1430-3
26 I. R. Cisneros-Contreras, A. L. Muñoz-Rosas, and A. Rodríguez-Gómez: Results Phys. **15** (2019) 102695. https://doi.org/10.1016/j.rinp.2019.102695

About the Authors

Yun Ho received her B.S. degree from National Kaohsiung University of Science and Technology, Taiwan, where she is currently studying for her M.S. degree. Her research interests include TCO thin films, materials engineering, and sensors.

Tao-Hsing Chen received his B.S. degree from National Cheng Kung University, Taiwan, in 1999, and his M.S. and Ph.D. degrees from the Department of Mechanical Engineering, National Cheng Kung University, in 2001 and 2008, respectively. From August 2008 to July 2010, he was a postdoctoral researcher at the Centre for Micro/Nano Science and Technology, National Cheng Kung University. In August 2010, he became an assistant professor at National Kaohsiung University of Applied Sciences (renamed National Kaohsiung University of Science and Technology), Taiwan. Since 2016, he has been a professor at National Kaohsiung University of Science and Technology. His research interests include metal materials, TCO thin films, thermal sensors, and photosensors. (thchen@nkust.edu.tw)